39th AIAA/ASME/SAE/ASEE Joint Propulsion Conference & Exhibit
Huntsville, Alabama
July 20-23, 2003

AIAA-2001-3671

A PLASMOID THRUSTER FOR SPACE PROPULSION

Syri J. Koelfgen* and Clark W. Hawk†
University of Alabama in Huntsville (UAH)
Propulsion Research Center
S225 Technology Hall
Huntsville, AL 35899

Richard Eskridge,‡ James W. Smith§ and Adam K. Martin¶
NASA Marshall Space Flight Center (MSFC)
Propulsion Research Center, TD40
Huntsville, AL 35812

ABSTRACT

There are a number of possible advantages to using accelerated plasmoids for in-space propulsion. A plasmoid is a compact plasma structure with an integral magnetic field. They have been studied extensively in controlled fusion research and are classified according to the relative strength of the poloidal and toroidal magnetic field (B_p and B_t, respectively). An object with $B_p / B_t \gg 1$ is classified as a Field Reversed Configuration (FRC); if $B_p \approx B_t$, it is called a Spheromak. The plasmoid thruster operates by producing FRC-like plasmoids and subsequently ejecting them from the device at a high velocity. The plasmoid is formed inside of a single-turn conical theta-pinch coil. As this process is inductive, there are no electrodes. Similar experiments have yielded plasmoid velocities of at least 50 km/s, and calculations indicate that velocities in excess of 100 km/s should be possible. This concept should be capable of producing Isp's in the range of 5,000 – 15,000 s with thrust densities on the order of 10^5 N/m^2. The current experiment is designed to produce jet powers in the range of 5 - 10 kW, although the concept should be scalable to several MW's. The plasmoid mass and velocity will be measured with a variety of diagnostics, including internal and external B-dot probes, flux loops, Langmuir probes, high-speed cameras and a laser interferometer. Also of key importance will be measurements of the efficiency and mass utilization. Simulations of the plasmoid thruster using MOQUI, a time-dependent MHD code, will be carried out concurrently with experimental testing.

INTRODUCTION

High specific-impulse engines are needed for large Δv space missions.[1] Furthermore, relatively high thrust allows for greater mission flexibility. A plasmoid thruster has many potential advantages for these missions. Since plasmoids are formed inductively in a Field Reversed Configuration (FRC),[2] they do not suffer from the electrode erosion losses inherent in many advanced propulsion concepts. Due to this electrode-less operation, the device is not limited to specific propellants. As the FRC is a self-contained plasmoid, it is not connected to the walls by magnetic field lines and thus does not require a magnetic nozzle. Consequently, the problem of detachment is lessened or possibly eliminated. Insulation of the plasma from the walls of the device also leads to a higher temperature than that of wall-supported plasmas. In addition, the FRC is relatively free of impurities that would otherwise cool the plasma through line-radiation.

---

* AIAA Student Member, NASA MSFC Graduate Student Researchers Program Fellow & UAH Graduate Research Assistant
† AIAA Fellow, Director of UAH Propulsion Research Center and Professor of Mechanical & Aerospace Engineering
‡ AIAA Member, NASA MSFC Aerospace Systems Engineer
§ NASA MSFC Mechanical Engineer
¶ NASA MSFC Physicist

Moreover, this high plasma temperature positively affects efficiency. Plasma resistivity is proportional to $T_e^{-3/2}$, so a high temperature plasma has a low resistivity (η), and therefore a high magnetic Reynolds number, $R = \mu_0 v L/\eta$, where μ_0 is the permeability of free space, v is the plasma velocity, and L is a characteristic scale length. Thus it may be possible to accelerate the plasmoids with high efficiency.

There are, on the other hand, several technological requirements that must be met for successful operation of a plasmoid thruster. Pulsed plasmoid formation requires rep-rates of 10 hertz or greater.[3] The device would therefore require low-voltage (i.e. less than 20 kV) formation and acceleration technology such as solid-state switches, or high-voltage (10 - 40 kV) switches and high energy density capacitors. Much improvement is required over existing technology for the in-space operation of a plasmoid thruster. The potential advantages however make it a worthy candidate for study. FRC's are empirically well understood, as they have been studied for years as a fusion core.[4]

PLASMOID THRUSTER EXPERIMENT (PTX)

A plasmoid is an object with an internal magnetic field structure. If the plasmoid has only toroidal current and poloidal magnetic field, it is called a Field Reversed Configuration (FRC); if both the current and magnetic field have poloidal and toroidal components, the plasmoid is classified as a Spheromak (Figure 1).[2] In practice there is a continuum between the two. The Plasmoid Thruster Experiment (PTX) produces FRC plasmoids in a theta-pinch formation chamber (Figure 2). The plasmoids are produced in a quartz tube situated inside of a theta-pinch coil. The solid aluminum coil has a conical half-angle of 17.5° and provides a peak magnetic field of 5 kGauss. The quartz tube is connected to a rectangular vacuum chamber for exhausting the plasmoids.

Four cylinders with internal permanent magnets surrounding the vacuum chamber are used to generate a bias field. Before firing, the chamber is filled with gas through the quartz tube. The gas is preionized by a high-voltage DC power supply that is connected between the gas inlet and the chamber (ground). A current pulse is then sent through the theta-pinch coil to produce a reversed magnetic field, i.e. a field in the opposite direction of the bias field. The coil is driven by a 640 nF, 40 kV capacitor bank which is switched with a Perkin-Elmer spark-gap. The bank is fired by sending an optical trigger signal to a high-voltage pulser that then triggers the spark-gap switch. The capacitors and their associated circuitry sit inside of a tank filled with mineral oil to prevent arcing. When triggered, the spark-gap switch closes, allowing the capacitor bank to discharge through the coil.

In the current experiment, only single FRC's are made. If the concept proves out, the experiment will be upgraded to burst mode operation.

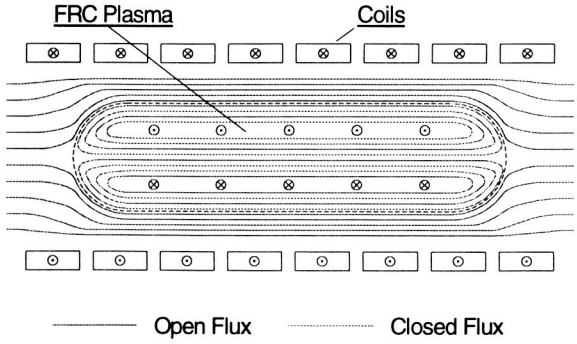

1(a) Field Reversed Configuration (FRC)

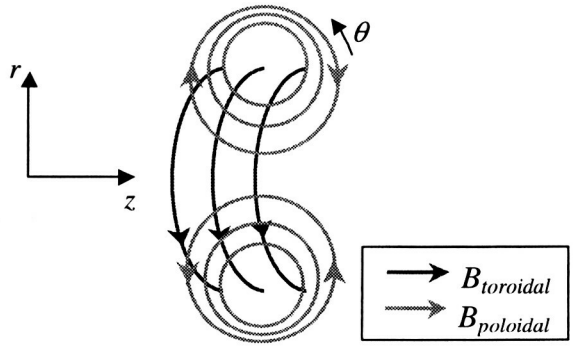

1(b) Spheromak

Figure 1. Plasmoid Magnetic Field Structure

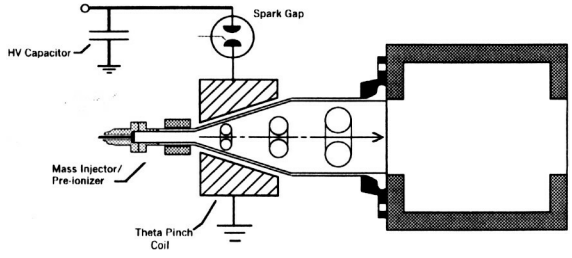

Figure 2. Plasmoid Thruster Experiment (PTX) Schematic

EXPERIMENTAL OPERATION

The PTX plasmoids are formed as FRC's in a theta-pinch coil as described previously. Typically, separate capacitor banks are used for pre-ionization, bias-field generation, and reversed field generation (compression).[2] PTX uses one bank to perform all three stages of formation. This method is referred to as first/second half-cycle formation (Figure 3). This technique was used in the earliest days of FRC research and has the virtue of being relatively simple.

The capacitor bank and coil constitute an L-C circuit, which rings sinusoidally. To begin operation, the gas is first introduced. A static fill is being used at present, but the system is being upgraded to incorporate gas-puff valves. The circuit is then closed with a high-current, high-voltage spark-gap switch, causing the capacitor to discharge through the coil. At time t_0 the axial magnetic field changes rapidly. This creates an electric field that pre-ionizes the plasma. Simultaneously, the plasma is seeded with the B-field produced during the first half-cycle. When the current/field swings through zero, the chamber contains a cold, partially ionized plasma with an imbedded magnetic field. As the field increases in the opposite direction, the plasma is shock heated to full-ionization and is compressed.

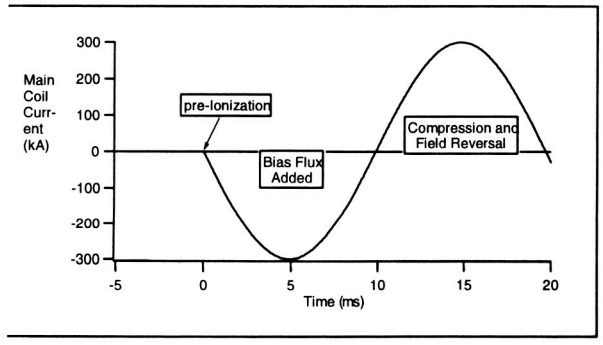

Figure 3. Ideal Coil Current for First/Second Half-Cycle Formation

SPICE was used to simulate the PTX circuit using assumed circuit component values of 640 nF capacitance, 194 nH external inductance, 60 mΩ external resistance, 28 nH coil inductance, and 35 kV charging voltage. The peak coil current generated was predicted by SPICE to be 53.4 kA at the quarter-cycle time $t_{1/4}$ = 0.6 ms (Figure 4). When the PTX capacitor bank was actually discharged through the theta-pinch coil, 32 kV of charging voltage was used, resulting in a peak quarter-cycle current of 28 kA (Figure 5), which was lower than predicted by SPICE.

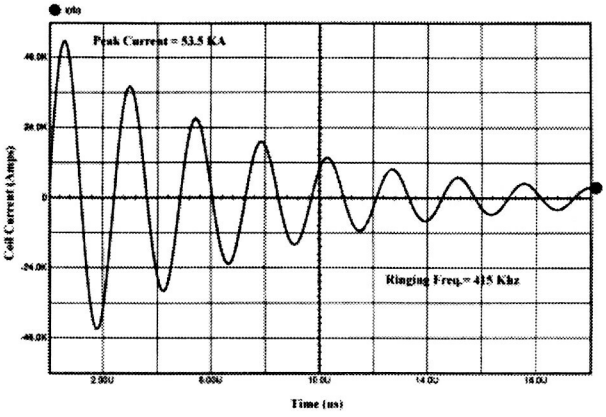

Figure 4. PTX Circuit Simulation using SPICE

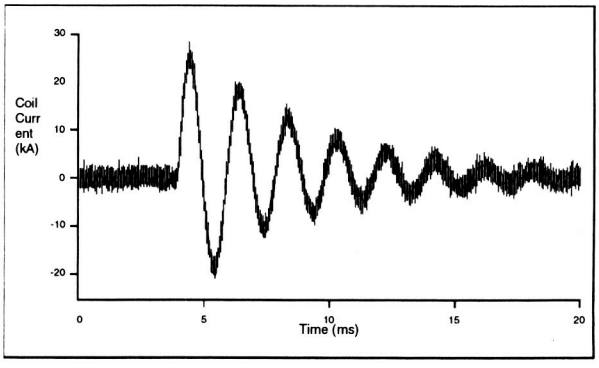

Figure 5. Actual PTX Capacitor Bank Discharge

DIAGNOSTICS

A variety of diagnostics will be used to study the formation and acceleration of the FRC plasmoids.

Excluded Flux Array

A singular feature of the FRC is that simple external magnetic diagnostics provide detailed information about the internal conditions of the plasma. In equilibrium, the FRC plasmoid sits inside of an open, solenoidal magnetic field; the boundary surface between the open and closed field lines is called the separatrix. FRC's are typically highly prolate, and this is characterized by an elongation *E*,

$$E = \frac{l_{sep}}{2r_{sep}} \tag{1}$$

where l_{sep} and r_{sep} are the length and radius of the separatrix respectively. The shape of the separatrix is typically found to be either elliptical, corresponding to a high pressure on the open field lines, or race-track like, corresponding to a low pressure on the open field lines. For a sufficiently prolate FRC, there is a simple formula, the Barnes relation, that links the plasma β (the ratio of the plasma pressure to magnetic field pressure) and the separatrix radius by the equation:

$$\langle \beta \rangle = \frac{\langle nk(T_e + T_i) \rangle}{\left(\frac{B_{wall}^2}{2\mu_0} \right)} = 1 - \frac{1}{2} X_s^2 \tag{2}$$

with

$$X_s = \frac{r_{sep}}{r_{coil}} \tag{3}$$

where n is the plasma density, k is Boltzmann's constant, T_e and T_i are the electron and ion plasma temperatures respectively, B_{wall} is the magnetic field at the vacuum wall and r_{coil} is the radius of the theta-pinch coil.

The separatrix radius is measured using an excluded flux array, which consists of a flux-loop[5] and associated B-dot probe[5,6] located beneath every coil, just outside of the vacuum wall (the quartz tube). (Figure 6) The B-dot probe measures B_{wall} and the flux loop measures the flux within that loop, where flux is given by

$$\Phi = \pi \left(r_{wall}^2 - r_{sep}^2 \right) B_{wall} \tag{4}$$

The flux within the separatrix is zero by definition. One then defines an 'excluded flux', $\Delta\Phi$, from:

$$\Delta\Phi = \pi r_{wall}^2 B_{wall} - \Phi = \pi r_{wall}^2 B_{wall} - \pi \left(r_{wall}^2 - r_{sep}^2 \right) B_{wall} = \pi r_{sep}^2 B_{wall} \tag{5}$$

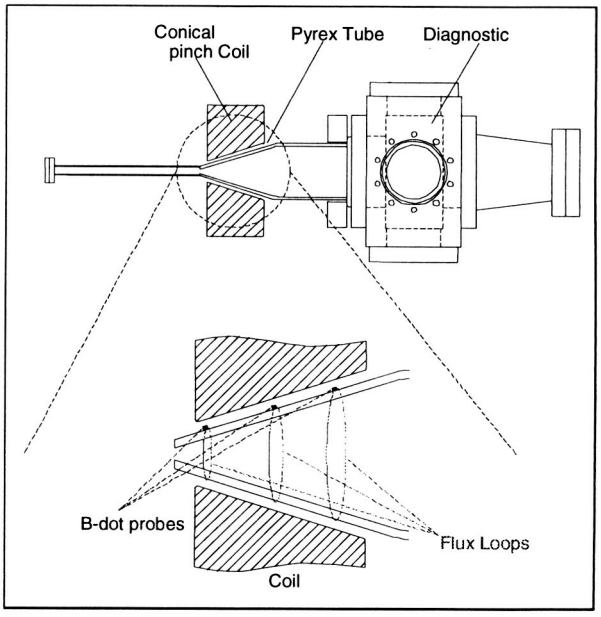

Figure 6. Excluded Flux Array

so that:

$$r_{sep} = \sqrt{\frac{\pi r_{wall}^2 B_{wall} - \Phi}{\pi B_{wall}}} \tag{6}$$

where r_{wall} is the radius to the vacuum wall. Hence, from the two independent measurements of B_{wall} and Φ, r_{sep} can be measured at every axial probe/flux-loop location, giving an axial profile of r_{sep}, and therefore the shape of the separatrix, as well as the internal plasma pressure from the Barnes relation.

Internal B-dot Probes

Internal B-dot probes[5,6] will be used to measure the magnetic fields in the open flux region, in the exhaust region, and within the FRC itself. Six sets of two B-dot probes (for a total of twelve probes) have been constructed for measuring B_z and B_θ, the axial and azimuthal magnetic fields, respectively, of the translating plasmoid. (Figure 7) The probes were wound with 36 gauge magnet wire around a 3.15 mm square form made from G-10 circuit board material. During construction of the probes, the fragile wire was kept taut by winding it around spools mounted to an optics table.

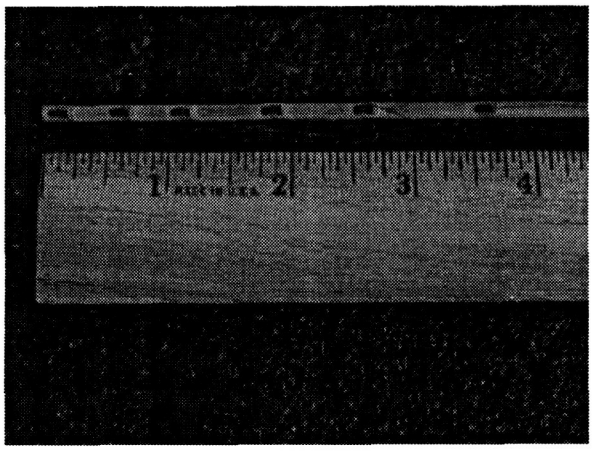

Figure 7. Internal B-dot Probes

A Helmholtz coil (Figure 8) was built for the purpose of calibrating the B-dot probes. The Helmholtz coil is a set of two coaxial current loops with equal radii, separated from each other by that radius. The radius of the PTX Helmholtz coil loops is 2.5 inches.

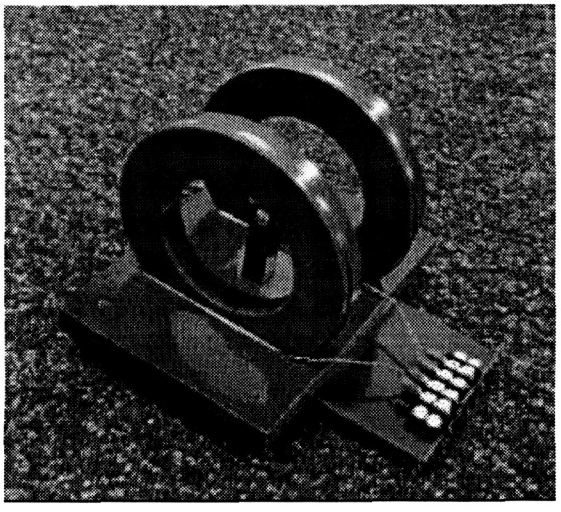

Figure 8. Helmholtz Coil

Equal currents flow in the same direction in each of the current loops. The magnetic field produced by the Helmholtz coil is extraordinarily uniform inside the volume of the coils, hence it provides a valuable calibration device. The Helmholtz coil magnetic field was calibrated with a power supply (current source), multimeter and Hall probe. The magnetic field inside the coils along the "z" axis is shown in figure 9. The measured data is not completely flat in the area of the uniform field, probably due to the fact that the coils were heating up during calibration and changing the effective current. Figure 10 shows the calibration data for the Helmholtz coil.

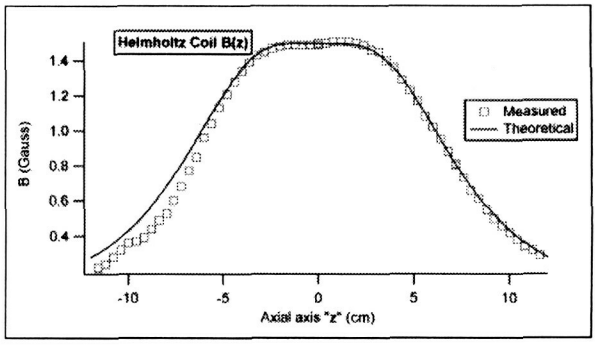

Figure 9. Axial Magnetic Field of Helmholtz Coil

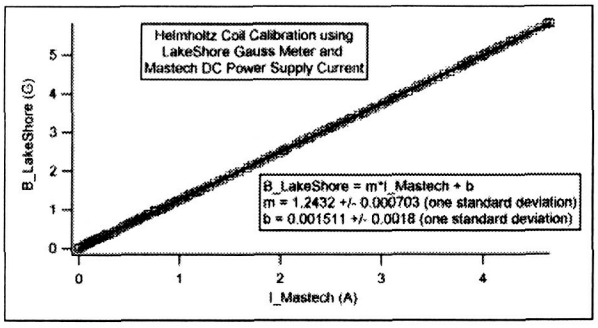

Figure 10. Helmholtz Coil Calibration Curve

In order to calibrate the B-dot probes, the Helmholtz coil was pulsed with a 300 VDC trigger, and the resulting voltage (translated into current and then magnetic field) responses of the Helmholtz coil and B-dot probes were measured with a digital oscilloscope. The magnetic field B seen by the B-dot probe is obtained through the relation

$$B = \int \dot{B} dt = \frac{1}{NA} \int V dt \qquad (7)$$

where $\dot{B}$ (B-dot) is the change in magnetic field with time, i.e. $\frac{\partial B}{\partial t}$, as measured by the probe, dt is the time of measurement, N is the number of turns of the probe, A is the cross-sectional area of

the probe, and V is the voltage measured across the leads of the probe.

The calibrated item, NA, was found to be within ~80% of the predicted value of NA = 10*(3.15 mm)^2 = 9.92E-5 m^2 for the probes. The frequency response of the B-dot probes was also assessed by applying a sine wave to the Helmholtz coil at frequencies from 1 kHz to 3 MHz. Responses of the Helmholtz Coil and the B-dot probes were measured with the oscilloscope. Figure 11 shows a typical plot of the calibration constant NA.

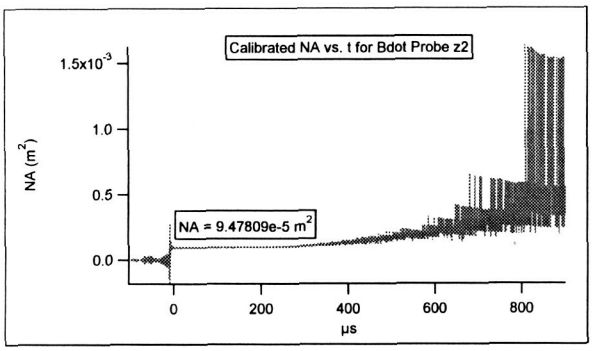

Figure 11. Typical B-dot Probe Calibration Plot

Langmuir Probes

Quadruple Langmuir probes[7] will be used to make local measurements of electron temperature T_e and number density n_e in the open flux region and in the exhaust region. Three of the four probes on the quadruple probe sample the Current-Voltage characteristic, and from this yield measurements of T_e and n_e. The fourth bent probe provides an estimate plasma velocity.

Interferometry

A heterodyne, quadrature He-Ne laser-interferometer will be used to measure the plasma number density in the FRC. This instrument is described briefly in Reference 8.

In laser interferometry, the laser beam is split into two beams of approximately equal intensity. One, called the scene-beam passes through the plasma; the other, called the reference beam, passes outside of the vacuum chamber. The scene beam acquires a phase-shift due to the plasma given by

$$\Delta\varphi = \frac{e^2\lambda}{4\pi\varepsilon_0 m_e c^2}\int n dl \qquad (8)$$

where e and m_e are the charge and mass of the electron respectively, ε_0 is the permittivity of free space, c is the speed of light, λ is the wavelength of the laser light, and n is the plasma number density (electron number density). The phase shift is proportional to the line-integral of the plasma density along the scene beam.

The reference beam is frequency-shifted by 40 Mhz using an acousto-optic Bragg cell. The scene and reference beams are recombined at a photo-detector and the resulting voltage signal is AC-coupled to an analyzer-circuit. There, the signal passes through a filter that selects the difference frequency. The interference signal (phase shift) is encoded as a frequency modulation of the 40 Mhz carrier signal. This 'heterodyning' preserves the sense of the phase shift when it goes through zero, and makes the instrument relatively insensitive to electrical noise and variations in amplitude.

The analyzer-circuit splits the interference signal into two signals. One of these signals is mixed with the original 40 Mhz carrier signal, and the other is mixed with the carrier signal shifted by 90°. These are then low-pass filtered, yielding two signals proportional to $\sin(\Delta\phi)$ and $\cos(\Delta\phi)$ respectively. From these, $\Delta\phi$ may be reconstructed unambiguously. The line-averaged density is then calculated from this phase-shift. At least 3, and perhaps as many as 6 chords of interferometry will be available for PTX.

High-speed Photography

High-speed photography will be used to image the FRC end-on, and to measure its velocity as it is translated. A variety of cameras with nanosecond resolution are available for the high-speed photography. PTX has access to a Cordin 220B camera that can take 8 pictures at 100 million frames/second, a Hamamatsu streak-camera and two Princeton Instruments PI-Max cameras, which have an intensified CCD array (512 x 512 pixels) and shutter-times down to 2 ns.

Bolometry

A silicon XUV photo-diode bolometer[6] will be used to measure the integrated radiation flux from the plasma, which will be instrumental in determining the overall energy balance.

EXPERIMENTAL OBJECTIVES

In order to have a high efficiency in a working device, it will be necessary to efficiently ionize the plasma and form the FRC. As with all electric propulsion systems, ionization represents a large frozen-flow loss in a plasmoid thruster.[1,2] It is necessary to reduce its overall influence on the system energy budget. With the theta-pinch formation method, the plasma is formed in a partially ionized state and is fully ionized during the shock heating caused by the field reversal. It has been found though that FRC equilibrium is sensitive to the pre-ionization.[5] Various pre-ionization techniques for PTX will be investigated, including ringing magnetic field ionization, coaxial plasma injectors, and perhaps rotating magnetic fields (RMF).

For a practical system, it will also be necessary to minimize resistive losses in the coils (by, for example, liquid nitrogen cooling), and to maximize the recapture of inductive energy in the coils and transmission line.

To evaluate the performance of the plasmoid thruster, measurements used to assess specific impulse, thrust and efficiency will be taken. Since propulsion performance is also characterized by how much of the plasma exits from the device, detachment of the plasmoid from the magnetic field lines will also be investigated. Similar experiments have yielded plasmoid velocities of at least 50 km/s, and calculations indicate that velocities in excess of 100 km/s should be possible. The concept should be capable of producing Isp's in the range of 5,000 – 15,000 seconds with thrust densities on the order of 10^5 N/m^2. The current experiment is designed to produce jet powers in the range of 5 - 10 kW, although the concept should be scalable to several MW's.

Isp-related measurements to be obtained include velocity and mass utilization. Velocity will be measured by use of high-speed photography, the internal B-dot probe array, laser interferometry and the quadruple Langmuir probe. Mass utilization will be evaluated by taking an inventory of the propellant mass put into the device compared to the mass of the plasma coming out. The mass of the plasma emerging from the device will be determined by measuring the density and volume of the ejected plasmoid. Density will be measured using the quadruple Langmuir probe and the laser interferometer. The Langmuir probe will provide a local measurement of electron number density, while the interferometer will make a non-intrusive measurement of line-averaged plasma density. The volume of the plasmoid will be determined by using the internal B-dot probe array as well as the high-speed photography.

Thrust-related measurements to be obtained include plasmoid mass and velocity. The mass and velocity will be acquired as previously described. Overall jet power, and therefore also thrust, will be limited by the rate at which the system can be fired. Currently, the experiment is being fired in single-shot mode, however upgrades to repetitive operation are being developed. Gas-puff valves operable at frequencies of up to 500 hz are being installed. For pulsed operation, it is also necessary to design capacitor banks and switching circuits that can be repetitively fired. This will be done after initial experiments are performed.

One of the advantages of the FRC thruster is that it should behave almost like a mass-driver, ejecting a magnetized plasmoid that is not magnetically attached to the nozzle. It will be necessary however to actually demonstrate this experimentally. Detachment of the plasmoid from the magnetic field lines will be investigated by characterizing how much of the plasmoid plasma stays attached to the field lines with increasing distance from the theta-pinch coil. Magnetic diagnostics and high-speed photography will be used to evaluate the shape and magnetic field structure of the translating plasmoid. In addition to the internal B-dot probe array, an excluded flux array will also be used to this means. It may also be favorable to allow the plasmoid to decay just as it reaches the nozzle (by making $\tau_{flux\ decay}$ comparable to $\tau_{transit}$), so as to recoup, at least partially, the frozen-in magnetic and plasma energy, and convert it into directed kinetic energy in the exhaust.

Simulations of the plasmoid thruster using MOQUI, a time-dependent MHD code, will be carried out concurrently with experimental testing.

INITIAL RESULTS

Images of PTX translating plasmoids have been captured with the Cordin camera. Figure 12 shows a plasmoid propagating in air at 43 mTorr backfill pressure. The Cordin camera has 8 CCD cameras in a circular configuration that take photos at a rate of 100 million frames/second, with a gate time of 10 ns per frame. The plasmoid velocity has been estimated from the Cordin images by assessing the amount of time for the plasmoid to traverse the vacuum chamber viewport over the 8 frames. The plasmoid shown

in Figure 12 (which was frame 6 of the 8) was estimated to have a velocity of 5.3 km/s.

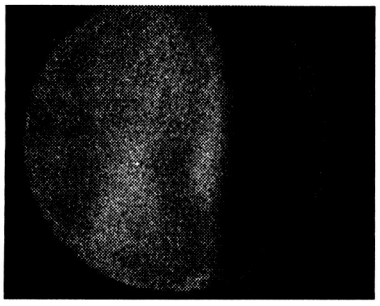

Figure 12. Translating Plasmoid

In order to begin evaluating PTX ionization, the Cordin camera has also been placed at the end of the vacuum chamber so that it is looking into the throat of the theta-pinch coil. For the 6% H_2 in He gas, a 128 mTorr static fill and preionization, a plot of plasmoid images (with a camera shutter speed of 20 ns) correlated with the coil current trace was made (Figure 13). From this plot it is proposed that two separate plasmoids are formed during a test firing.

CONCLUSION

The plasmoid thruster is a promising concept for in-space propulsion with a number of possible advantages. The Plasmoid Thruster Experiment seeks to evaluate the concept. The plasmoid thruster operates by producing FRC-like plasmoids in a theta-pinch coil and subsequently ejecting them from the device at a high velocity. To evaluate the performance of PTX, the plasmoid mass, mass utilization, velocity and thruster efficiency will be measured with a variety of diagnostics, including internal and external B-dot probes, flux loops, Langmuir probes, high-speed cameras and a laser interferometer.

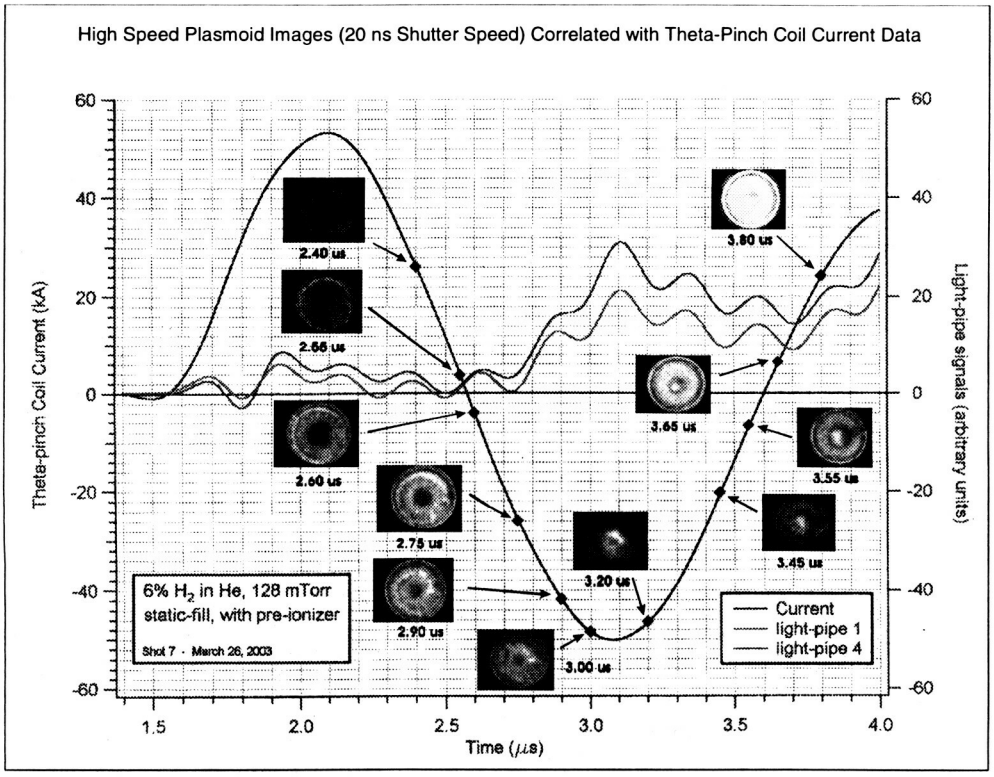

Figure 13. Plasmoid Images with Coil Current

REFERENCES

1.) "Physics of Electric Propulsion," Robert G. Jahn, *McGraw-Hill*, 1968.

2.) "Field Reversed Configurations – Review Paper," M. Tuszewski, *Nuclear Fusion* **28**(11), 1988.

3.) "Pulsed High-Density Fusion Rocket," J. Slough, *NASA Fusion Propulsion Workshop*, Nov. 8-10, 2000, NASA Marshall Space Flight Center, Huntsville, Alabama.

4.) "Inductive Field-Reversed Configuration Accelerator for Tokamak Fueling," A.L. Hoffman et. al., *Fusion Technology*, **36**, Sep. 1999.

5.) "Principles of Plasma Diagnostics," I. H. Hutchinson, *Cambridge University Press*, 1987.

6.) "Plasma Diagnostic Techniques," Richard H. Huddlestone and Stanley L. Leonard, *Academic Press*, 1965.

7.) "Application of a Quadruple Probe Technique to MPD Thruster Plume Measurements," R. L. Burton and S. Del Medico, *Journal of Propulsion and Power* **9**(5), pp. 771-777, Sep. – Oct. 1995.

8.) "Photographic, magnetic, and interferometric measurements of current sheet canting in a pulsed plasma accelerator" T.E. Markusic, E.Y. Choueiri, 37th *AIAA/ASME/SAE/ASEE Joint Propulsion Conference & Exhibit, July 8-11, 2001, Salt Lake City, Utah,* AIAA Paper 2001-3896.

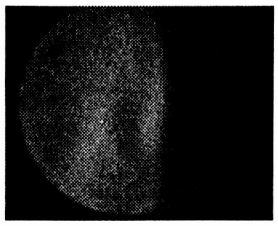

A Plasmoid Thruster for Space Propulsion

Syri J. Koelfgen, NASA MSFC GSRP Fellow
University of Alabama in Huntsville
Propulsion Research Center
39th AIAA/ASME/SAE/ASEE Joint Propulsion Conference & Exhibit
July 20-23, 2003
Huntsville, Alabama

Experimental Team

NASA Marshall Space Flight Center / TD40:
Dr. Adam Martin, Richard Eskridge, Mike Lee, James Smith, Tommy Reid, Jeff Richeson

University of Alabama in Huntsville:
Syri Koelfgen, Dr. Clark Hawk

Presentation Outline

I. Background
II. Plasmoid Propulsion
III. Plasmoid Thruster Experiment (PTX)
IV. Diagnostics
V. Imaging Results
VI. Future Work

Propulsion System Comparison

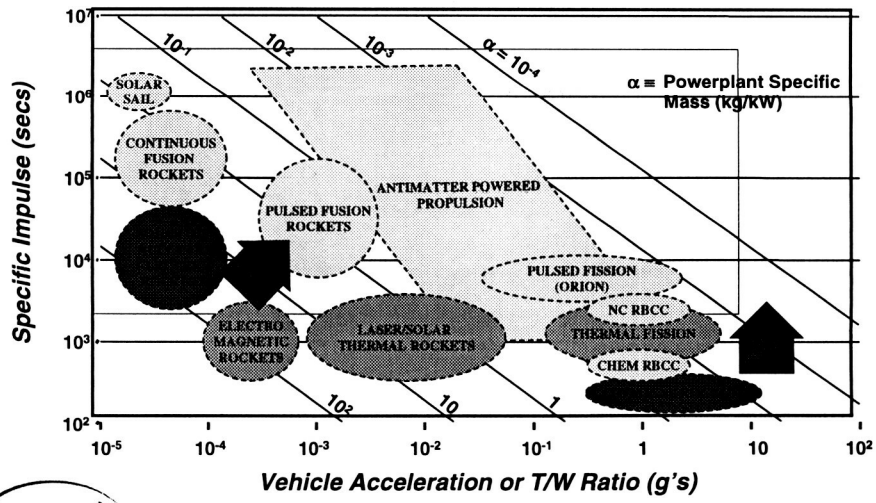

Compact Toroids (Plasmoids)

- A Compact Toroid is a plasma w/ a self-contained magnetic field structure (i.e., a magnetized plasmoid)
  a) If it has only toroidal current and poloidal magnetic field, it is called a Field Reversed Configuration (FRC)
  b) If both the current and the magnetic field have both toroidal and poloidal components, it is called a Spheromak
- In practice, there is a continuum between the two

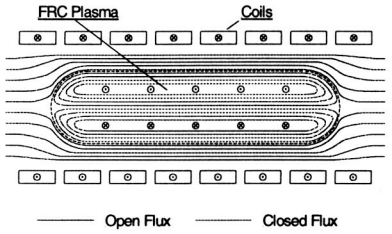

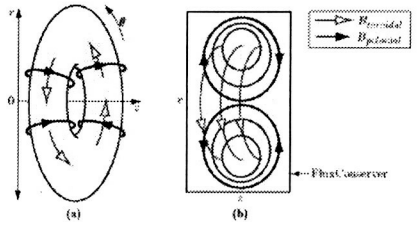

(a) Field Reversed Configuration **(b) Spheromak**

UAH Propulsion Research Center

UAH University of Alabama in Huntsville

Theta-Pinch (FRC) Plasmoid Formation

- FRC plasmoids formed with a theta-pinch coil
- Propelled to high velocity in acceleration stage by compressing the B field behind it
  - v = 20 – 100 km/s;
  - Isp = 5,000 – 15,000 s
- Thrust determined from plasma density and rep-rate (subject to power constraints)
- Initially single plasmoids made; later upgrade to burst mode operation

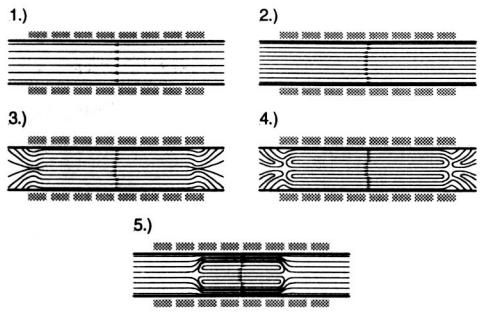

UAH Propulsion Research Center

UAH University of Alabama in Huntsville

Plasmoid Propulsion

- FRC-produced plasmoids formed repetitively & magnetically accelerated
- No electrodes (inductive formation)
- Potential performance:
  - Jet Power: 10 kW – MW's
  - Specific Impulse: 5,000–15,000 s
  - Efficiency: 50–80 %
- Potential applications:
  - Low power (P_{JET} < 100 kW), high specific impulse (I_{SP} > 5,000 s) missions
  - High power (P_{JET} ~ MW's), high specific impulse missions

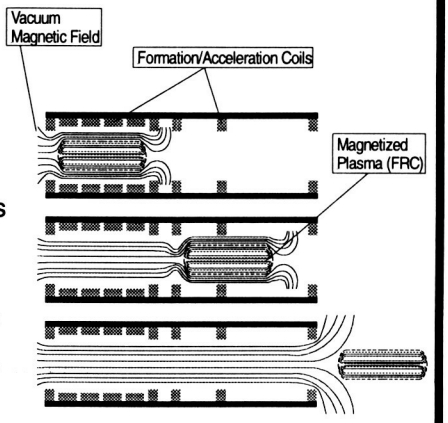

UAH University of Alabama in Huntsville

Plasmoid Propulsion Advantages & Requirements

Advantages

- High Isp (5,000–15,000 s)
- High thrust density
  - $P_{chamber} = 10^5 – 10^6$ Pa
- No electrodes (inductive formation)
- Plasma exhaust contained by internal magnetic field (aiding in detachment)
- FRC's are empirically well understood – the technology draws on results routinely obtained in FRC fusion research
- FRC's have been accelerated to 250 km/s – yielding an "I_{sp}" equivalent of 25,000 s
- Potentially scalable to high powers (up to MW's)

Technological Requirements

- Pulsed plasmoid formation requires:
  - Rep-rates > 10 hz
- Recapture of inductive energy
- Either:
  - Low-voltage (< 20 kV) formation and acceleration technology: solid-state switches

    or
  - High-voltage (10-40 kV) switches, and high energy-density capacitors
- Much improvement required over existing technology

UAH University of Alabama in Huntsville

Plasmoid Thruster Experiment (PTX)

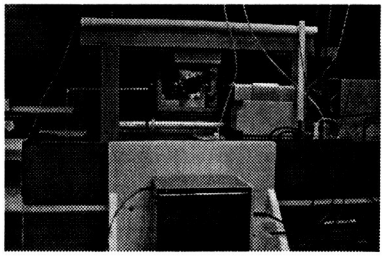

PTX Side View

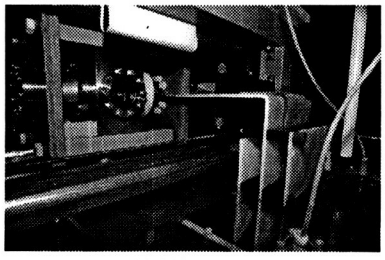

PTX Oblique View

PTX Schematic:

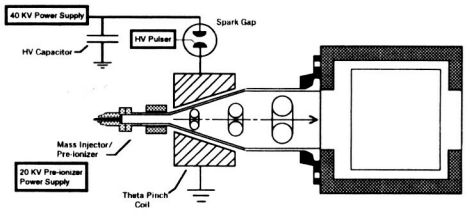

UAH Propulsion Research Center

UAH University of Alabama in Huntsville

Plasmoid Thruster Experiment (PTX)

θ-Pinch Coil (Above), Coil & Pyrex Tube (Below)

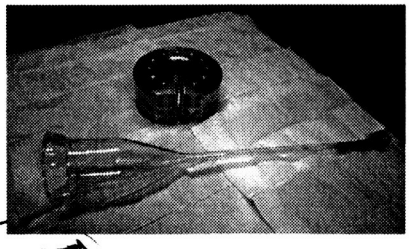

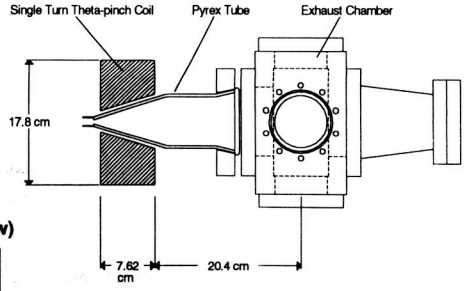

PTX Coil, Tube & Vacuum Chamber; Coil half-angle = 17.5°

UAH Propulsion Research Center

UAH University of Alabama in Huntsville

Plasmoid Thruster Experiment (PTX)

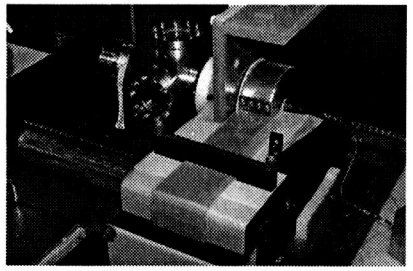

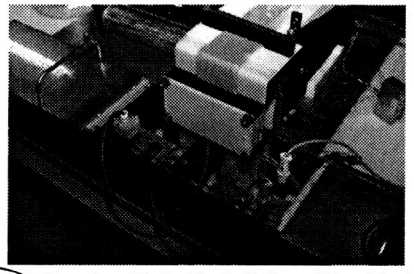

Chamber, Theta-Pinch Coil, and Bus (Top)
Capacitors etc. in Oil Tank (Bottom)

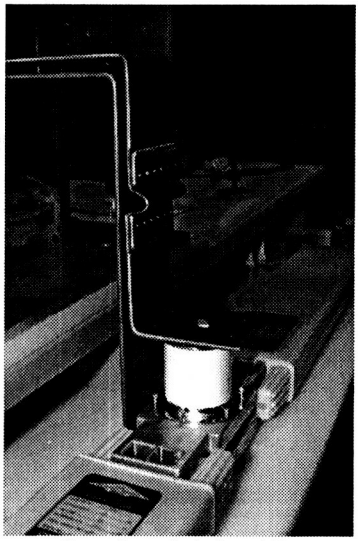

Capacitors, Switch and Bus

UAH University of Alabama in Huntsville

Plasmoid Thruster Experiment (PTX)

SPICE Simulation of PTX Coil/Bank

C = 640 nF
L_{ext} = 194 nH
L_{coil} = 35 nH
R_{ext} = 60 mΩ
V_{charge} = 28 kV
$t_{1/4}$ = 0.6 ms
I_{PEAK} = 53.5 kA

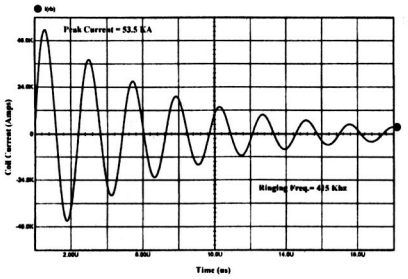

Firing of PTX Capacitor Bank

- PTX Capacitor bank discharged thru θ-pinch coil
- Charge voltage = 32 kV, Peak current = 28 kA - lower than predicted by SPICE

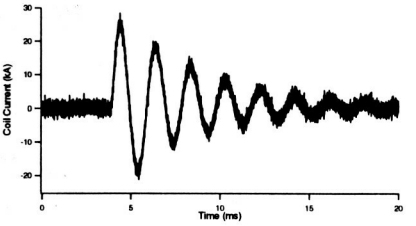

UAH University of Alabama in Huntsville

PTX Diagnostic Tools

- **Excluded Flux Array**
  - Axial array of flux loops and B-dot probes that measures plasmoid separatrix radius
- **Internal B-dot Probes**
  - Measure shape and internal magnetic field structure of translating plasmoids
- **Quadruple Langmuir Probe**
  - Takes local measurements of T_e and n_e as well as plasma flow velocity
- **Interferometry**
  - Heterodyne, quadrature He-Ne laser interferometer measures line-averaged n_e
- **High-Speed Photography** for imaging plasmoids in exhaust chamber
  - PI-Max gated CCD cameras
  - Hamamatsu Streak Camera
  - Cordin Camera - takes 100 Million frames per second

Excluded Flux Array

Axial array of flux loops and B-dot probes measures r_s (separatrix radius) along compact toroid:

$$F = B\,p(r_l^2 - r_s^2)$$

For a prolate, cylindrically symmetric compact toroid (FRC), the volume averaged β may be found from:

$$\langle\beta\rangle = 1 - r_s^2 / (2\,r_c^2)$$

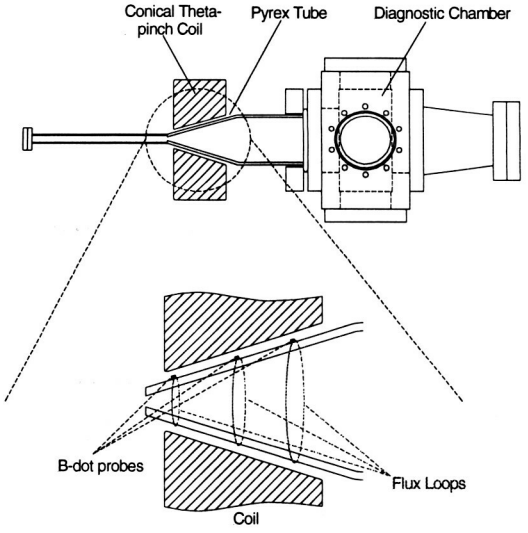

Internal B-dot Probes

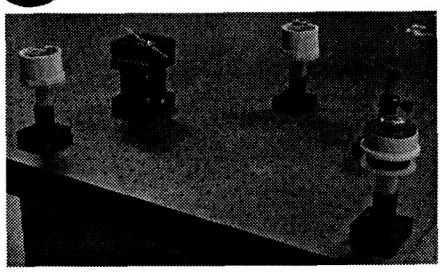

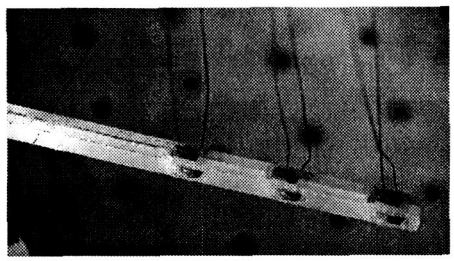

- **Internal B-dot Probes:**
- 6 Sets of 2 B-dot Probes (12 total) for measuring B_z and B_θ of translating plasmoid
- Probes wound with 36 gauge magnet wire
- 10 turns, Form Cross-Sectional Area ~ $(3.15\ mm)^2$

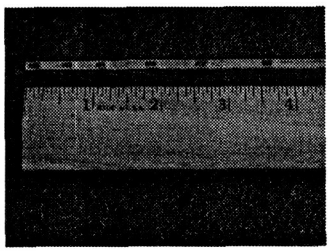

UAH University of Alabama in Huntsville

Internal B-dot Probes – Calibration w/ Helmholtz Coil

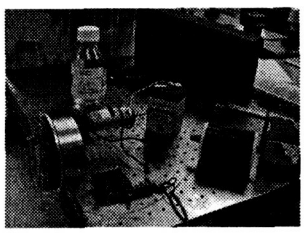

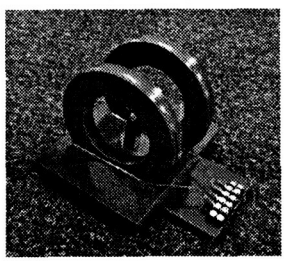

Helmholtz Coil – 18 gauge magnet wire, Radius = 2.5 in., Winding (Above Left), Completed Coil (Above Right)

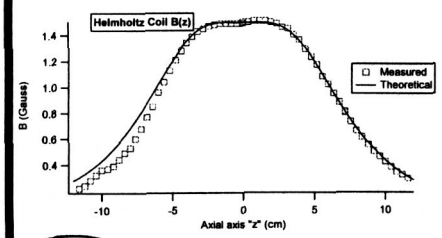

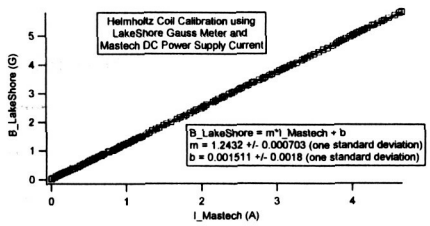

Helmholtz Coil Calibration, B(z) (Above Left), B(I) (Above Right)

UAH University of Alabama in Huntsville

Internal B-dot Probes - Calibration

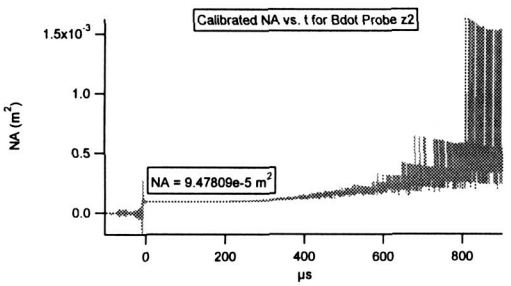

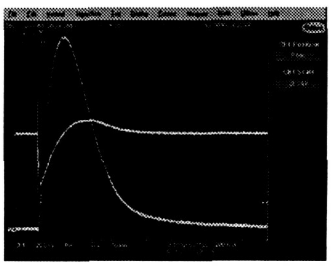

- Calibration of Internal B-dot Probe NA's (number of windings • area) with Helmholtz Coil
  - Pulsed Helmholtz Coil with 300 VDC; Measured Helmholtz Coil and B-dot Probe response with oscilloscope
  - NA's within ~80% of predicted NA of 10*(3.15 mm)^2 = 9.92E-5 m^2
- Frequency response calibration
  - Sine wave input to Helmholtz Coil for 1 kHz – 3 MHz

UAH Propulsion Research Center

UAH University of Alabama in Huntsville

High-Speed Photography

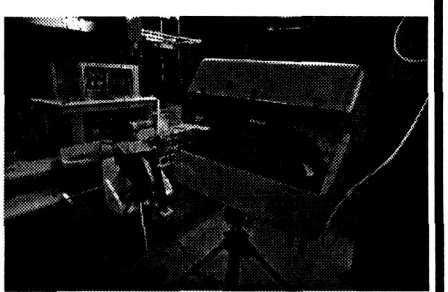

Hamamatsu C7700 Optical Streak Camera

• Captures high velocity plasma front motion

Cordin model 220B Framing Camera:

• 8 CCD cameras in circular configuration take up to 100 million frames per second, 8 frames total
• Gate time: 10 ns per frame
• Camera placed at side of chamber (shown above) and at end of chamber

UAH Propulsion Research Center

UAH University of Alabama in Huntsville

Translating Plasmoid

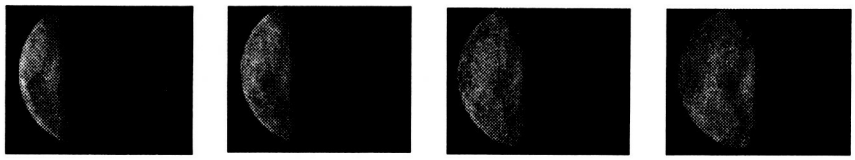

21 us 22 us 23 us 24 us

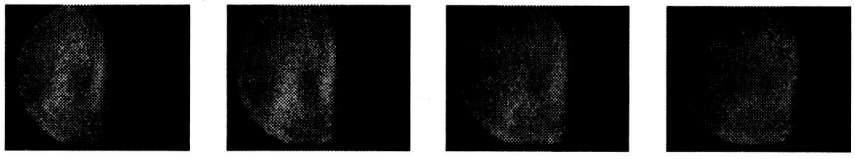

25 us 26 us 27 us 28 us

Propagating plasmoid in Air at 43 mTorr backfill pressure (view from side of vacuum chamber); Velocity for this test was 5.3 km/s

UAH University of Alabama in Huntsville

Translating Plasmoid

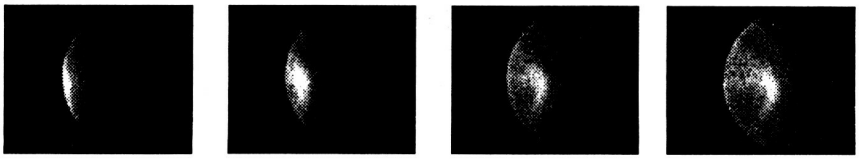

10.0 us 10.5 us 11.0 us 11.5 us

12.0 us 12.5 us 13.0 us

Side view of plasmoid propagating into backfill taken with Cordin 220B framing camera. Center of image is 20.4 cm downstream of theta-pinch coil. Gas conditions: 6% H_2 in He, at 95 mTorr. Times indicated are from start of discharge. Images are consistent with a plasmoid traveling at hypersonic velocity.

UAH University of Alabama in Huntsville

Plasmoid Images

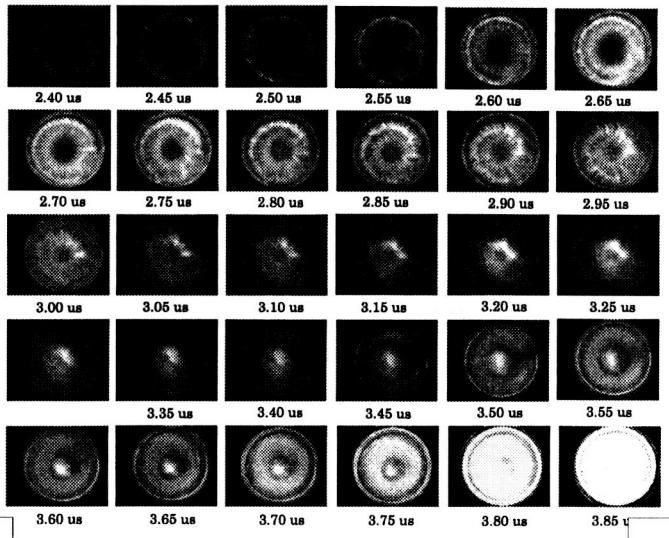

Time development of plasmoid (looking into throat of θ-pinch coil). Coil current 53.5 kA. Exposure time 20 ns, time between frames 50 ns. Pressure = 125 mTorr. Gas: 6% H2 in He

Plasmoid Images Along Current Trace

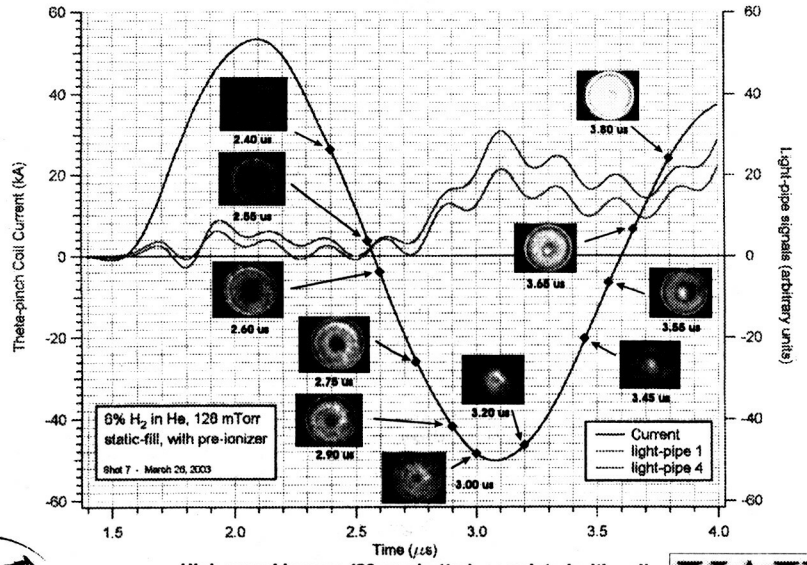

High speed images (20 ns shutter) correlated with coil current data for plasmoid test shot on March 26, 2003

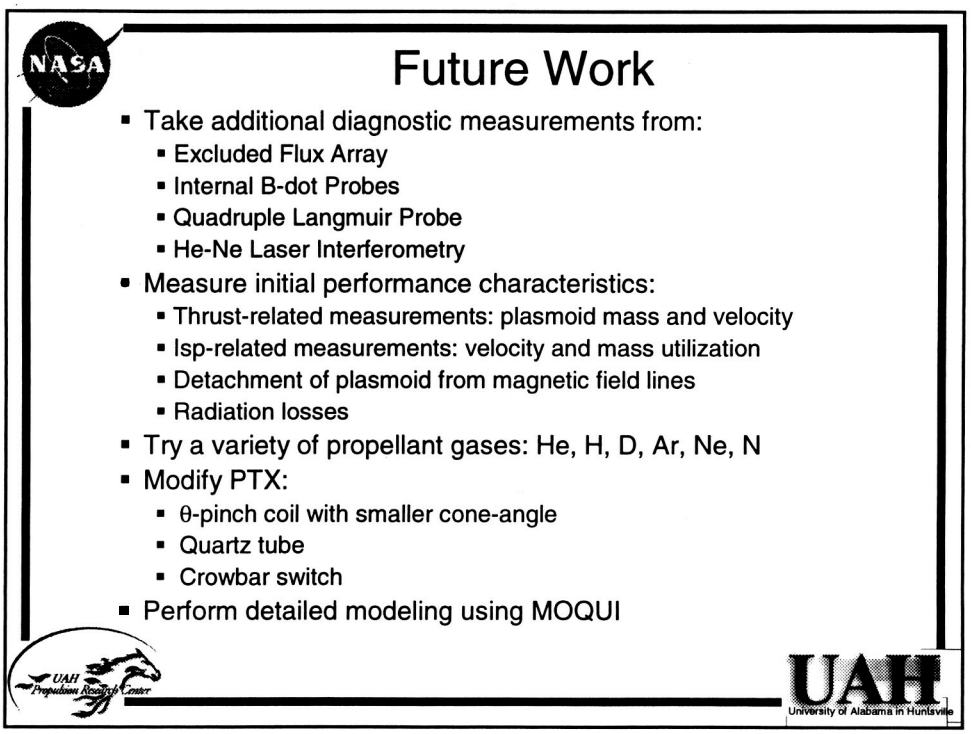
NASA
Future Work
Take additional diagnostic measurements from:
Excluded Flux Array
Internal B-dot Probes
Quadruple Langmuir Probe
He-Ne Laser Interferometry
Measure initial performance characteristics:
Thrust-related measurements: plasmoid mass and velocity
Isp-related measurements: velocity and mass utilization
Detachment of plasmoid from magnetic field lines
Radiation losses
Try a variety of propellant gases: He, H, D, Ar, Ne, N
Modify PTX:
θ-pinch coil with smaller cone-angle
Quartz tube
Crowbar switch
Perform detailed modeling using MOQUI
UAH Propulsion Research Center
UAH
University of Alabama in Huntsville